The abts and sulp families of anion transporters from Caenorhabditis elegans

Teresa Sherman, Marina N. Chernova, Jeffrey S. Clark, Lianwei Jiang, Seth L. Alper and Keith Nehrke

Am J Physiol Cell Physiol 289:341-351, 2005. First published Apr 6, 2005;
doi:10.1152/ajpcell.00071.2005

Am J Physiol Cell Physiol 289: C341–C351, 2005.
First published April 6, 2005; doi:10.1152/ajpcell.00071.2005.

The *abts* and *sulp* families of anion transporters from *Caenorhabditis elegans*

Teresa Sherman,[1] Marina N. Chernova,[3,5] Jeffrey S. Clark,[3,5] Lianwei Jiang,[3,5] Seth L. Alper,[3,4,5] and Keith Nehrke[1,2]

[1]*Departments of Medicine (Nephrology Unit) and* [2]*Pharmacology & Physiology, University of Rochester Medical Center, Rochester, New York;* [3]*Molecular and Vascular Medicine Unit and* [4]*Renal Division, Beth Israel Deaconess Medical Center, Boston;* [5]*Department of Medicine, Harvard Medical School, Boston, Massachusetts*

Submitted 4 February 2005; accepted in final form 30 March 2005

Sherman, Teresa, Marina N. Chernova, Jeffrey S. Clark, Lianwei Jiang, Seth L. Alper, and Keith Nehrke. The *abts* and *sulp* families of anion transporters from *Caenorhabditis elegans*. *Am J Physiol Cell Physiol* 289: C341–C351, 2005. First published April 6, 2005; doi:10.1152/ajpcell.00071.2005.—The *slc4* and *slc26* gene families encode two distinct groups of gene products that transport HCO_3^- and other anions in mammalian cells. The *SLC4* and *SLC26* proteins are important contributors to transepithelial movement of fluids and electrolytes and to cellular pH and volume regulation. Herein we describe the cDNA cloning from the nematode *Caenorhabditis elegans* of four anion bicarbonate transporter (*abts*) homologs of *slc4* cDNA and eight sulfate permease (*sulp*) homologs of *slc26* cDNA. Analysis of transgenic nematode strains carrying promoter::GFP fusions suggests relatively restricted expression patterns for many of these genes. At least three genes are expressed primarily in the intestine, three are expressed primarily in the excretory cell, and one is expressed in both of these polarized cell types. One of the genes is also expressed exclusively in the myoepithelium-like cells of the pharynx. Many of the *sulp* gene products localize to the basolateral membrane rather than to the apical membrane. Several ABTS and SULP proteins exhibited anion transport function in *Xenopus* oocytes. The strongest Cl^- transporter among these also mediated Cl^-/HCO_3^- exchange. These findings encourage exploitation of the genetic strengths of the nematode model system in the study of the physiological roles of anion transport by the proteins of these two highly conserved gene families.

ANION EXCHANGERS (AE) play a key role in the maintenance of many physiological processes in the body. The two main AE gene families encoding transporters of HCO_3^- as well as other anions are the *SLC4* and *SLC26* families. The mammalian AEs *SLC4A1–SLC4A3* encode proteins that mediate Na^+-independent electroneutral exchange of Cl^- for HCO_3^-. AE1/SLC4A1 was first identified as the erythrocyte band 3 protein (30, 48, 57), with AE2/SLC4A2 and AE3/SLC4A3 then identified by homology (see Ref. 29). These three proteins comprise a subfamily of the wider SLC4 family, which includes the Na^+-dependent HCO_3^- transport proteins SLC4A4–SLC4A11 (for review, see Refs. 2, 47).

AE1/SLC4A1 is the principal integral membrane protein of the erythrocyte. In concert with carbonic anhydrase, it participates in CO_2 metabolism and pulmonary gas exchange (56). AE1 is also expressed in the basolateral membrane of the acid-secreting intercalated cell of the kidney collecting duct. AE1 mutations are associated with spherocytic anemia and distal renal tubular acidosis (1). AE1 also plays an important role in mitotic cytokinesis during the proliferative steps of late erythroid development (45). AE2/SLC4A2 is found in many tissues and, unlike AE1, is inhibited by protons in the physiological range and activated by hypertonicity, suggesting a role in intracellular pH (pH_i) homeostasis and cell volume regulation (19–21, 23, 60). Absence of AE2/SLC4A2 in the mouse leads to gastric abnormalities and achlorhydria, with death occurring at or before weaning (13). Human mutations of the electrogenic Na^+-HCO_3^- cotransporter (NBC) isoform 1 (NBCe1)/SLC4A4 are associated with severe proximal renal tubular acidosis with ocular abnormalities (22). The electroneutral Na^+-HCO_3^- cotransporter 1 (NBCn1)/SLC4A7-knockout mouse exhibits blindness and auditory impairment (5). RNA interference (RNAi) gene knockdown of the borate transporter 1 (BTR1)-electrogenic Na^+-coupled borate transporter 1 (NaBC1)-SLC4A11 in cultured human cells inhibits [^{3}H]thymidine uptake in a manner that can be rescued by borate supplementation (43).

The SLC26 anion transporter family encodes polypeptide products of at least 10 genes (for review, see Ref. 37). The original mammalian member of this family, the sulfate anion transporter (SAT-1/SLC26A1), was expression cloned as a sulfate transporter (4). Additional family members were identified by positional cloning of disease loci for diastrophic dysplasia sulfate transporter (DTDST/SLC26A2) (17), congenital Cl^--losing diarrhea [downregulated in adenoma (DRA)/SLC26A3] (18, 54), and Pendred syndrome (pendrin/SLC26A4) (12), as well as by genomic homology searches (32). The SLC26 AEs exhibit a wide range of anion selectivity. DTDST/SLC26A2 appears to mediate HCO_3^--inhibitable sulfate transport (51). Pendrin/SLC26A4 exchanges I or Cl^- for Cl^- or HCO_3^- but can also transport formate. SLC26A3 is primarily a Cl^-/HCO_3^- exchanger, whereas SLC26A6 transports a broad range of anions, including oxalate (26, 65). Their mechanisms of transport remain controversial (7, 27), and prestin/SLC26A5 may move bound intracellular anion through a portion of the transmembrane electrical potential without completing anion translocation and transrelease (42).

The apically localized SLC26 polypeptides SLC26A3/DRA, SLC26A4/pendrin, and SLC26A6 are upregulated by coexpressed CFTR (7, 8, 27). SLC26A3 conversely can upregulate CFTR channel activity through binding of its sulfate transporter and anti-σ-factor antagonist (STAS) domain to the R domain of CFTR (28). SLC26A3 is also thought to interact with CFTR (28) and with Na^+/H^+ exchanger 3 (NHE3) (31) indirectly through common interactions with postsynaptic density-95/*Drosophila* disk large/zonula occludens-1 homology

Address for reprint requests and other correspondence: K. Nehrke, Nephrology Unit, Dept. of Medicine, Medical Center Box 675, 601 Elmwood Ave., Rochester, NY 14642 (e-mail: keith_nehrke@urmc.rochester.edu).

The costs of publication of this article were defrayed in part by the payment of page charges. The article must therefore be hereby marked "*advertisement*" in accordance with 18 U.S.C. Section 1734 solely to indicate this fact.

(PDZ) domain proteins such as NHE regulatory factor (NHERF)/NHE3 kinase A regulatory protein (E3KARP).

We have previously cloned and characterized the entire family of nematode NHEs *nhx-1–nhx-9* (39) and have shown that loss of the intestine-specific *nhx-2* gene product leads to a starvation phenotype and increases longevity (38). Toward the goal of establishing *C. elegans* as an experimental system for the study of pH regulation in an intact animal, we have initiated characterization of putative *C. elegans* anion transporters homologous to mammalian Cl^-/HCO_3^- exchangers. Herein we present the cDNA sequences, cellular and subcellular localization, and initial functional studies of these novel proteins.

METHODS

cDNA cloning. Basic local alignment search tool (BLAST) analysis was performed with default parameters identified in the *C. elegans* genome database for predicted open reading frames (ORFs) homologous to human SLC4 proteins and eight predicted ORFs homologous to human SLC26 proteins. The *C. elegans* genes encoding the SLC4-related ORFs (followed in parentheses by the newly assigned gene names) are F52B5.1 (*abts-1*), F52D10.1 (*abts-2*), F57F10.1 (*abts-3*), and R03E9.3 (*abts-4*). The *C. elegans* genes encoding the SLC26-related ORFs are C55B7.6 (*sulp-1*), F14D12.5 (*sulp-2*), F41D9.5 (*sulp-3*), K12G11.1 (*sulp-4*), K12G11.2 (*sulp-5*), W01B11.2 (*sulp-6*), WO4G3.6 (*sulp-7*), and ZK287.2 (*sulp-8*). The 5′ and 3′ ends of each predicted cDNA were amplified using nested rapid amplification of cDNA ends (RACE) and anchored with either an adapter primer at the 3′ end (added during cDNA synthesis) or an SL1-transspliced leader primer at the 5′ end. Internal primers were based on conserved sequence motifs in the predicted proteins. Multiple products of both the predicted and nonpredicted sizes were cloned and sequenced for each RACE reaction to assess splice site variation as well as alternate transcriptional initiation and termination sites. Multiple attempts at 3′-RACE for *sulp-6* were unsuccessful. The physiological presence and integrity of each splice variant was confirmed by performing RT-PCR amplification of the full-length coding sequence, followed by sequencing of multiple amplification products on both strands and alignment with the nematode genome sequence. Single-site mutations were corrected using oligonucleotide-mediated mutagenesis. The full-length cDNA were submitted to both GenBank and WormBase.[1]

Promoter transgene analysis. As described previously (39), transcriptional promoter fusions to green fluorescent protein (GFP) were created by performing PCR amplification of a 4-kb 5′ upstream genomic sequence for each isoform and using restriction site-tagged oligonucleotide primers with a mutant start codon complement (ATG to TTG). These PCR products were cloned into the complementary sites of the five synthetic introns-containing vector pFH6.II (F. Hagen, University of Rochester, Rochester NY) derived from pPD95.81 (A. Fire, Carnegie Institution of Washington, Baltimore, MD) to create the four SLC4-related plasmids pFH6-abts-1–pFH6-abts-4 and the eight SLC26-related plasmids pFH6-sulp-1–pFH6-sulp-8. Translational promoter fusions (pTS1-abts-N and pTS1sulp-N) were amplified using 3′ genomic primers that annealed immediately before the stop codons to produce in-frame 3′ fusions with GFP. Because the *abts-4* gene exceeds 17 kb in length, the *abts-4* translational fusion was created with the cDNA rather than with the gene. In several instances, rather than clone the promoter/ORF, a PCR product containing GFP from pFH6.II was annealed with a promoter/ORF genomic PCR product with complementary overhangs, and the resulting amplified linear DNA was then injected as described below.

[1] The GenBank accession numbers are AY887903–AY887917 (*abts*) and AY954522–AY954525 (*sulp*).

GE24 *pha-1*(*e2123ts*) nematodes were cultured at 15°C on nematode growth medium plates containing 5 μg/ml cholesterol seeded with OP50 bacteria from an overnight culture using standard techniques. GFP fusion constructs were mixed with pCL1 at 75 μg/ml each in high-K^+ injection buffer to rescue the *pha-1* deficit (15) and then were coinjected into the gonad of young adults as described previously (34). After 4 days at 22°C, surviving first generation (F1) progeny from at least 10 injections were picked to separate plates to evaluate germline transmission. F2 generation nematodes anesthetized on 2% agarose pads were irradiated using a 150-W Hg lamp with a TILL Photonics Polychrome IV monochomator and a Nikon Eclipse E2000 microscope with Apo series objectives and a GFP long-pass emission filter set, or using a Leica DRME confocal microscope under 488-nm laser illumination and a fluorescein isothiocyanate filter set as appropriate. Images were processed using Adobe PhotoShop software (Adobe Systems, San Jose, CA).

Anion influx. The ORFs for *abts-1*, *abts-2*, *sulp-2*, and *sulp-4* were subcloned into the oocyte expression vector pBF (63). Capped cRNA was transcribed from linearized cDNA templates with SP6 RNA polymerase (Ambion, Austin, TX) and resuspended in diethylpyrocarbonate-treated water. RNA integrity was confirmed by performing agarose gel electrophoresis in formaldehyde. Mature female *Xenopus* (NASCO, Madison, WI) were maintained and subjected to partial ovariectomy under tricaine hypothermia anesthesia as previously described (20) and in conformity with methods approved by the Institutional Animal Care and Use Committee of the Beth Israel Deaconess Medical Center. *Stages 5* and *6* oocytes were manually defolliculated after incubation of ovarian fragments with 2 $mg \cdot ml^{-1}$ collagenase A or collagenase B (Boehringer Mannheim, Indianapolis, IN) for 60 min in ND-96, pH 7.4, containing (in mM) 96 NaCl, 2 KCl, 1.8 $CaCl_2$, 1 $MgCl_2$, and 5 HEPES (6). Oocytes were injected on the same day with 10 ng of cRNA in 50 nl of water or with the same volume of water. Injected oocytes were then maintained for 2–6 days at 19°C.

Unidirectional $^{36}Cl^-$ influx studies were performed for 60-min periods as previously described in ND-96 at pH 7.4. The [^{35}S]sulfate influx experiments were performed in 150 μl of influx medium containing 5 μCi carrier-free [^{35}S]sulfate (47 nM) in 0.1 mM unlabeled sulfate. The [^{14}C]oxalate influx experiments were performed in Ca^{2+}- and Mg^{2+}-free influx medium containing 0.5 mM oxalate (2.67 $\mu Ci \cdot ml^{-1}$).

Cl^-/HCO_3^- exchange measurements. Oocytes previously injected with *abts-1* cRNA or with water were incubated for 30 min at room temperature with 5 μM 2′,7′-bis-(2-carboxyethyl)-5-(and-6)-carboxyfluorescein acetoxymethyl ester (BCECF-AM). BCECF-labeled oocytes were mounted in a 0.8-ml superfusion chamber on a microscope stage. Cl^-/HCO_3^- exchange was measured using BCECF fluorescence ratio imaging of oocyte pH_i changes during removal and restoration of superfusate Cl^- concentration (72 mM) in the presence of 5% CO_2-24 mM HCO_3^-, with gluconate used as the substituting anion (11). Data acquisition and analysis were performed using MetaFluor software (Universal Imaging, Downingtown, PA). Initial rates of dpH_i/dt were measured using the least-squares linear fit of initial slopes. Buffer capacity (β_T) was calculated as the sum of intrinsic buffer capacity (β_i), which is 18–20 mM/pH unit (59), plus CO_2 buffer capacity (β_{CO_2}). Data are expressed as proton flux $J_{H^+} = dpH_i/dt \times \beta_T$.

RESULTS

The abts and sulp gene families in C. elegans. An initial BLAST analysis of the *C. elegans* genome revealed four putative genes encoding predicted polypeptides homologous to human SLC4 AE proteins and eight putative genes encoding polypeptide sequences homologous to human SLC26 AE proteins. Each of the initially predicted *C. elegans* ORFs was used to design multiple sets of nested primers for 5′ and 3′ RACE.

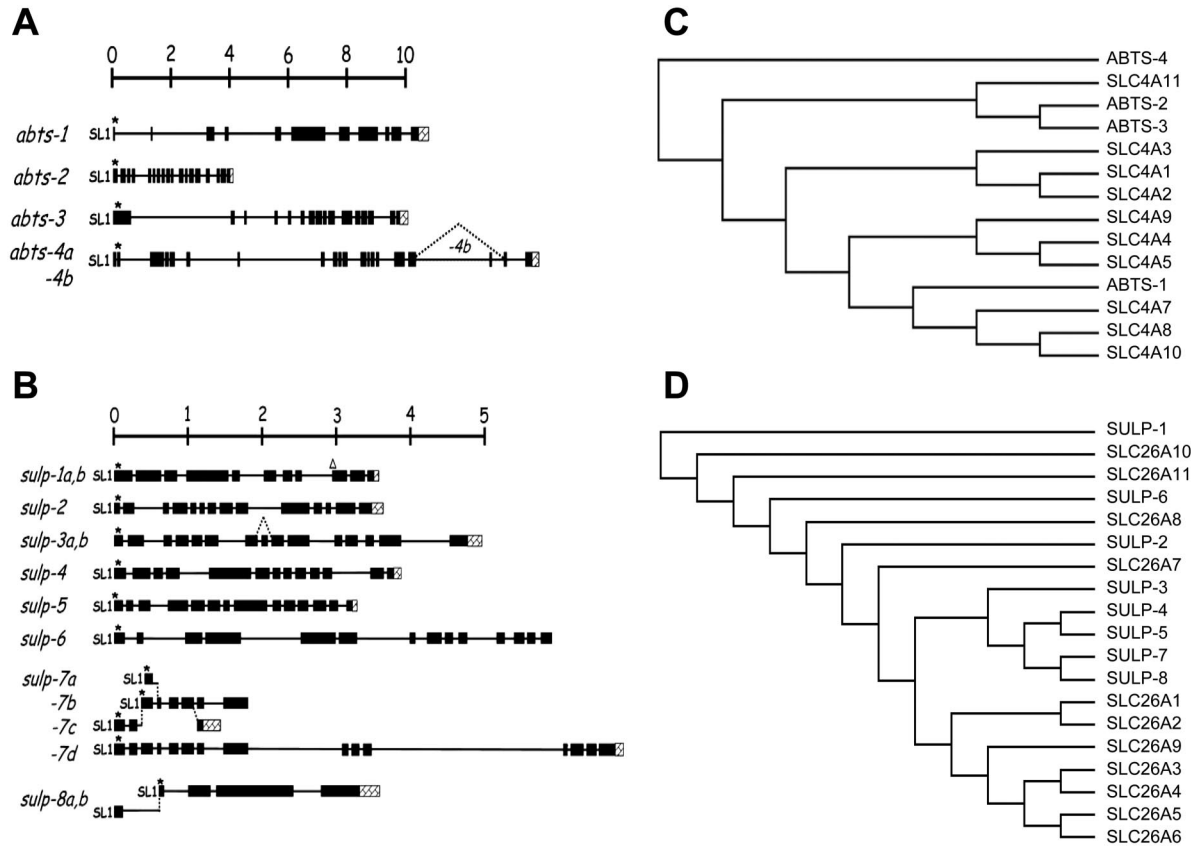

Fig. 1. Genomic structure of the anion bicarbonate transporter (*abts*) (*A*) and sulfate permease (*sulp*) (*B*) gene families. A ruler (in kb) is shown above each diagram. Coding exons are shown to scale as shaded boxes, start codons are indicated by an asterisk, and 3′ UTRs are represented by hatched boxes. SL1-transspliced leaders are indicated where appropriate. A splice substitution that occurred at ~25% frequency in the *abts-4* gene is depicted by a dashed line running from an alternative splice donor site 20 nt beyond the end of exon 17 to the splice acceptor site at the beginning of exon 19. A variable 12-nt deletion was identified at the start of exon 9 in ~50% of the cDNA obtained from *sulp-1*, while the loss of exon 8 was observed in one *sulp-3* clone. In addition, multiple short transcripts were identified from *sulp-7*. Finally, *sulp-8* gave rise to two alternate SL1-transspliced leader sites of addition, but the conceptually translated proteins of each were identical. To examine possible orthologs, CLUSTAL W multiple sequence alignments of the entire conceptually translated open reading frames (ORFs) were followed by phylogenetic analysis of the human *SLC4* with the worm *abts* genes (*C*) or of the human *SLC26* with the worm *sulp* genes (*D*).

The 5′ and 3′ end sequences identified by performing RACE were then used to amplify full-length ORFs using high-fidelity reaction conditions and *Pyrococcus furiosus* (*Pfu*) polymerase (Stratagene, La Jolla, CA). Each targeted region was amplified independently at least three times, and in cases in which multiple PCR products were obtained, each band was isolated, cloned, and sequenced. This approach generated complete cDNA for each of the four SLC4 homologs, anion bicarbonate transporters named *abts-1–abts-4*, and for six of the eight SLC26 homologs, sulfate permeases named *sulp-1–sulp-8*, as shown in Fig. 1, *A* and *B*. The 3′ end of the *sulp-6* transcript remains unknown, despite 3′-RACE amplification attempts with multiple sets of validated, nested PCR primer pairs. Although *sulp-7* amplification products encoded predicted ORFs that were much shorter in length than predicted by the other *sulp* genes, these short cDNA were polyadenylated. However, a recent addition to the nematode database suggests the existence of a longer isoform that we did not identify using 3′-RACE (see *sulp-7d* in Fig. 1*B*).[2]

These putative transporter polypeptides of the nematode resemble their mammalian counterparts in predicted membrane topography. The ABTS proteins consist of an NH_2-terminal cytoplasmic domain of 400–700 amino acids (aa), a transmembrane domain of 500 aa predicted to traverse the lipid bilayer 12–14 times, and a short COOH-terminal cytoplasmic domain. The *C. elegans* polypeptide sequences are in general more closely related to each other than to any of the mammalian gene products (Fig. 1*B*), with the exception of a recent addition to the *SLC4* superfamily: BTR1/SLC4A11 (44). BTR1 is a borate transporter important for cell proliferation (43) and is related more closely to the ABTS-2 and ABTS-3 proteins of *C. elegans* than to any other mammalian *SLC4* gene product. In addition, the ABTS-1 protein resembles the mammalian Na^+-dependent Cl^-/HCO_3^- exchangers SLC4A8 and SLC4A10 to a slightly greater degree than it resembles other mammalian sequences. Three of the four *abts* gene products (ABTS-1, -3, and -4) contain variants of a WRETARW motif that is well conserved in most human AE/NBC-type transporters and is important for the pH sensitivity of AE in rodent slc4a2 and slc4a3 (59). ABTS-1 and -4 also contain a conserved histidine ~20 aa further toward the COOH terminus that has likewise been shown to be important for pH sensing (60). All four

[2] During the preparation of this article, a new expressed sequence tag (EST) for *sulp-7* that encodes a predicted polypeptide of 582 amino acids, an expected length for a functional sulp family member, appeared in the database.

ABTS proteins also contain, near the COOH terminus, variations of an acidic region that in SLC4A1 and SLC4A2 binds carbonic anhydrase II (64), with resultant enhancement in HCO_3^- transport (11, 58).[3]

The predicted SULP protein sequences are 25–35% identical to their mammalian counterparts, with the greatest similarity evident in the hydrophobic predicted transmembrane domains. SULP-3, -4, -5, -7, and -8 polypeptides form a separate subclass within the SULP superfamily, but the low degree of homology with the mammalian SLC26 polypeptides renders ortholog assignment difficult.

All SULP proteins contain STAS domains (3), with the sole exception of the short *sulp-7* polypeptide variants. STAS domains of SLC26 proteins may contribute to plasma membrane localization (55), and previous work has shown that loss of this domain abolishes SLC26 transport activity. Loss or inactivating mutation of the STAS domain of SLC26A3 also abolishes stimulation of CFTR in overexpression systems (28). However, unlike the COOH-terminal class I PDZ-binding motifs of the mammalian SLC26 proteins, only SULP-1 among the eight SULP proteins has a predicted (class III) PDZ-binding motif (aa 726–729). Additional functionally significant amino acids conserved among mammalian and plant SLC26 proteins (24, 49) are present in the nematode proteins.

Several *sulp* splice variants were found. Two *sulp-1* exon 9 acceptor sites are separated by 12 nt, resulting in optional inclusion of four additional amino acids within a variable loop of the STAS domain (Fig. 1*C*). A *sulp-3* cDNA lacking exon 8 is missing amino acids that are highly conserved within a putative transmembrane domain, but an *SLC26A6* splice variant (SLC26A6-d) that contains a similar deletion was recently found to be functional (33), and hAE1 has been shown to retain activity in the absence of transmembrane domains 5 and 6 (16). *Sulp-7* gave rise to multiple 5′ and 3′ RACE products, while the two *sulp-8* variants differed at the 5′ UTR but encoded identical polypeptides. All *sulp* transcripts except *sulp-3* were found to be SL1 transspliced.

The abts and sulp genes are expressed in both unique and overlapping patterns. Genomic DNA fragments upstream of the mapped start sites for each member of the *abts* and *sulp* gene families were cloned into a promoterless GFP expression vector and then injected into nematodes to create transgenic strains that fluoresce in the cells in which each of the transporters is expressed. These expression patterns likely do not reveal the complete cellular range of expression. Strong GFP expression in one cell type may obscure weaker expression in another nearby cell. GFP transgene loss during cell division can result in mosaicism and an incomplete repertoire of fluorescent cells in any given animal. In addition, the expression of transgenes cannot be assumed to replicate accurately native gene expression patterns. However, with these caveats in mind, the gene expression patterns described herein can be used to direct efforts at elucidating physiologically relevant gene function. Table 1 summarizes the cellular patterns of gene expression described below.

Table 1. *Cellular expression pattern of promoter::GFP fusions*

Name	Fusion Type	Tissues
abts-1::GFP	Transcription	Neurons, hypodermal cells, pharynx, weakly in anal gland and intestine
abts-2::GFP	Transcription	Single posterior neuron
abts-3::GFP	Transcription	Neurons, hypodermal cells
abts-4::GFP	Transcription	Intestine, single pair of neurons in head
sulp-1::GFP	Transcription	Neurons, weakly in hypodermal, intestinal, and muscle cells
sulp-2::GFP	Transcription	Intestine, several neurons in head, rectal gland
sulp-3::GFP	Transcription	Pharynx
sulp-4::GFP	Transcription	Excretory cell
sulp-5::GFP	Transcription	Excretory cell
sulp-6::GFP	Transcription	Posterior intestine
sulp-7::GFP	Transcription	Hypodermal cells, body wall muscle, pharynx, intestine
sulp-8::GFP	Transcription	Excretory cell, intestine, rectal gland

GFP, green fluorescent protein; *abts,* anion bicarbonate transporter; *sulp*, sulfate permease.

Figure 2 shows representative images from transgenic nematodes expressing *abts* promoter::GFP transcriptional fusions. The *abts-1* promoter drove GFP expression primarily in neurons and hypodermal cells, but weak fluorescence also was observed in the pharynx and body wall muscle cells (Fig. 1*A*). The *abts-2* promoter expressed GFP in a single neuron in the tail ganglion (Fig. 1*C*). This pattern may indicate remarkable specificity but also may represent inappropriate expression of an incomplete gene. The *abts-3* gene fusion was expressed exclusively in neurons and hypodermal cells coincident with *abts-1* (Fig. 1*E*). The *abts-4* gene fusion was restricted to the intestine, with the highest expression observed in cells of the posterior- and anterior-most gut region (Fig. 1*G*).

Figure 3 presents images of strains expressing *sulp* promoter::GFP transcriptional fusions. Many *sulp* family promoters drove GFP expression in cells that function in the transepithelial movement of nutrients, electrolytes, and water, and multiple isoforms were often expressed in single cell types. For example, each of the *sulp-4*, *-5*, and *-8* fusions was strongly expressed in the excretory cell (Fig. 2). The H-shaped excretory cell consists of two symmetric canals running laterally, linked at the cell body, and connected to the environment via a duct and pore. In addition to expression in the excretory cell, the *sulp-8*::GFP transgene was coexpressed in intestinal cells with *sulp-2*, *sulp-6*, and *sulp-7* transgenes (Fig. 2).

The *sulp-1*::GFP fusion was expressed strongly in multiple neurons and weakly in hypodermal cells, the intestine, and body wall muscle in a pattern close to that of *abts-1* (Fig. 3*A*). The *sulp-3* promoter drove GFP expression exclusively in the pharyngeal muscles (Fig. 3*E*). The *sulp-7* transgene was widely expressed in body wall, pharyngeal, and vulval muscles, hypodermal cells of the body and head, and the intestine (Fig. 3*M*), but it was entirely absent from neurons.

To establish subcellular localization of the putative anion transporter proteins, we expressed translational GFP fusions for *abts-2* (single cell), *abts-4* (intestine), *sulp-2* (intestine), *sulp-4* (excretory cell), *sulp-5* (excretory cell), and *sulp-8*

[3] SL1-transsplice leaders were identified for all of the *abts* gene products, but several EST clones from *abts-3* that suggest the existence of two additional 5′ exons occurring >10 kb upstream, followed by a large intron and replacing exon 1 (to which the RACE primers were designed), have recently been described in WormBase. This would result in a protein predicted to be 162 amino acids shorter at the 5′ end (data not shown). This database information suggests that two alternate promoters may control transcription of the *abts-3* gene.

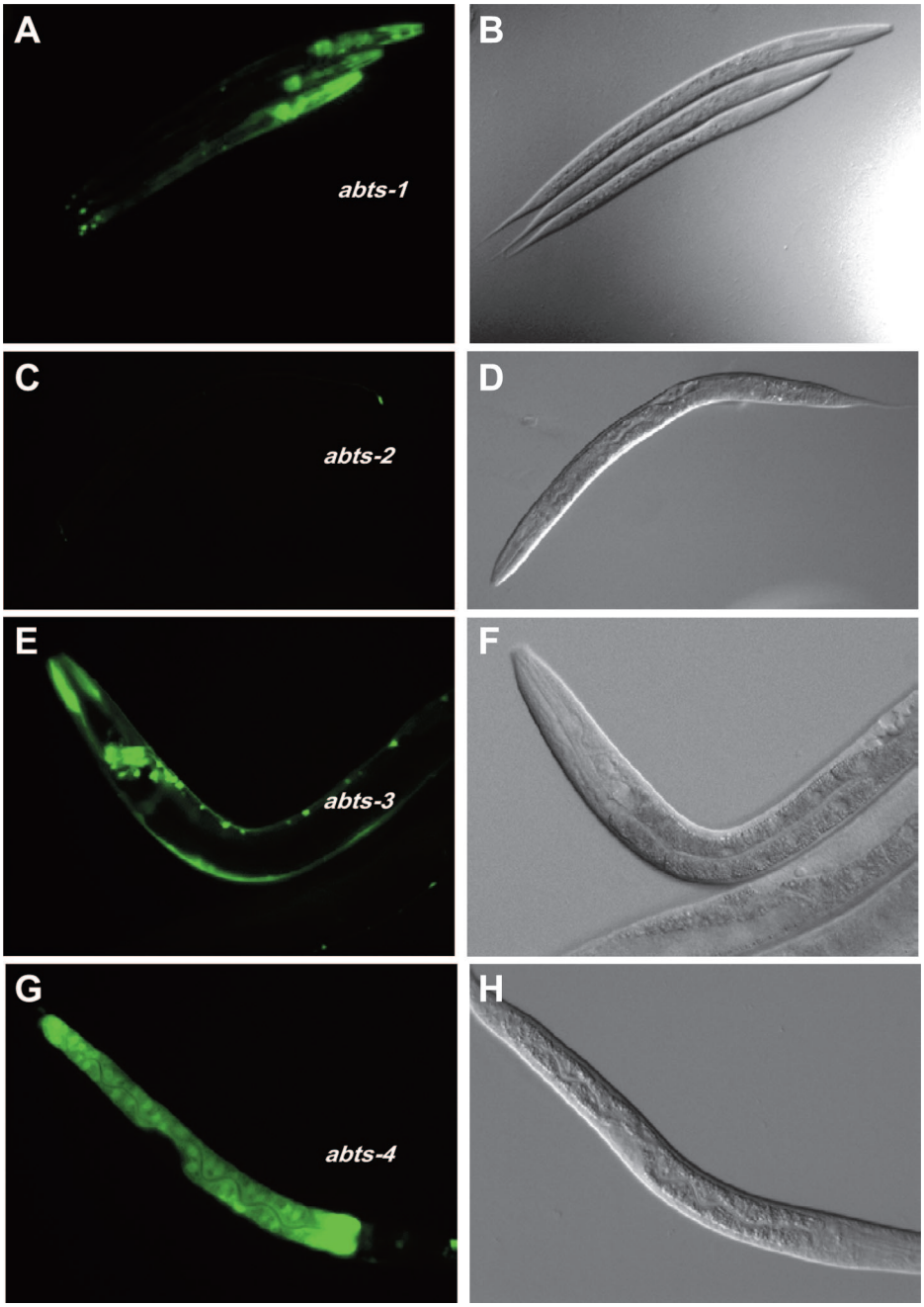

Fig. 2. Cell expression profiles of the *abts* gene family: transcriptional green fluorescent protein (GFP) fusions. Representative fluorescent and differential interference contrast images of lines expressing GFP from the *abts-1* (*A* and *B*), *abts-2* (*C* and *D*), *abts-3* (*E* and *F*), or *abts-4* (*G* and *H*) promoters. While the *abts-1* and *-3* promoters drove the expression of GFP in neurons and hypodermal cells (see Table 1), the expression of *abts-4* appeared to be restricted to the intestine and the expression of *abts-2* seemed to be restricted to a single neuron in the tail.

(intestinal and excretory cell). These fusions encompassed a genomic region consisting of the promoter and the entire ORF of the protein, with GFP attached in place of the natural stop codon. In the case of *abts-4*, the ORF was inserted as a cDNA fragment rather than as a genomic fragment, owing to vector size limitations. Table 2 summarizes the observed localizations of these fusion proteins.

Surprisingly, although expression of the *abts-2*::GFP transcriptional fusion was restricted to a single cell of the rectal ganglion, the *abts-2* translational fusion was strongly expressed in the excretory cell of larva (Fig. 4*A*). In addition, the ABTS-2::GFP fusion was expressed in the adult ovaries (Fig. 4*C*). This suggests that important promoter or enhancer elements of the *abts-2* gene were missing from the transcriptional fusion and likely reside within the first several introns. As was true for the *abts-4* transcriptional fusion, the *abts-4* translational fusion was expressed exclusively in the intestine, where it was localized to the basolateral membrane of the gut cells (Fig. 4*E*).

The SULP-4-, -5-, and -8::GFP translational fusion proteins were expressed, as expected, in the excretory cell, but with significantly different distributions (Fig. 5). The translational *sulp-4* fusion resided in apical canaliculae that probably serve to transport salts and fluid from the cytoplasm to the lumen of the excretory cell (Fig. 5*F*). In contrast, the *sulp-5* fusion was localized to punctate structures distributed irregularly along the excretory canals (Fig. 5*H*), and the *sulp-8* fusion was found at the basolateral membrane (Fig. 5*D*). SULP-8::GFP was also

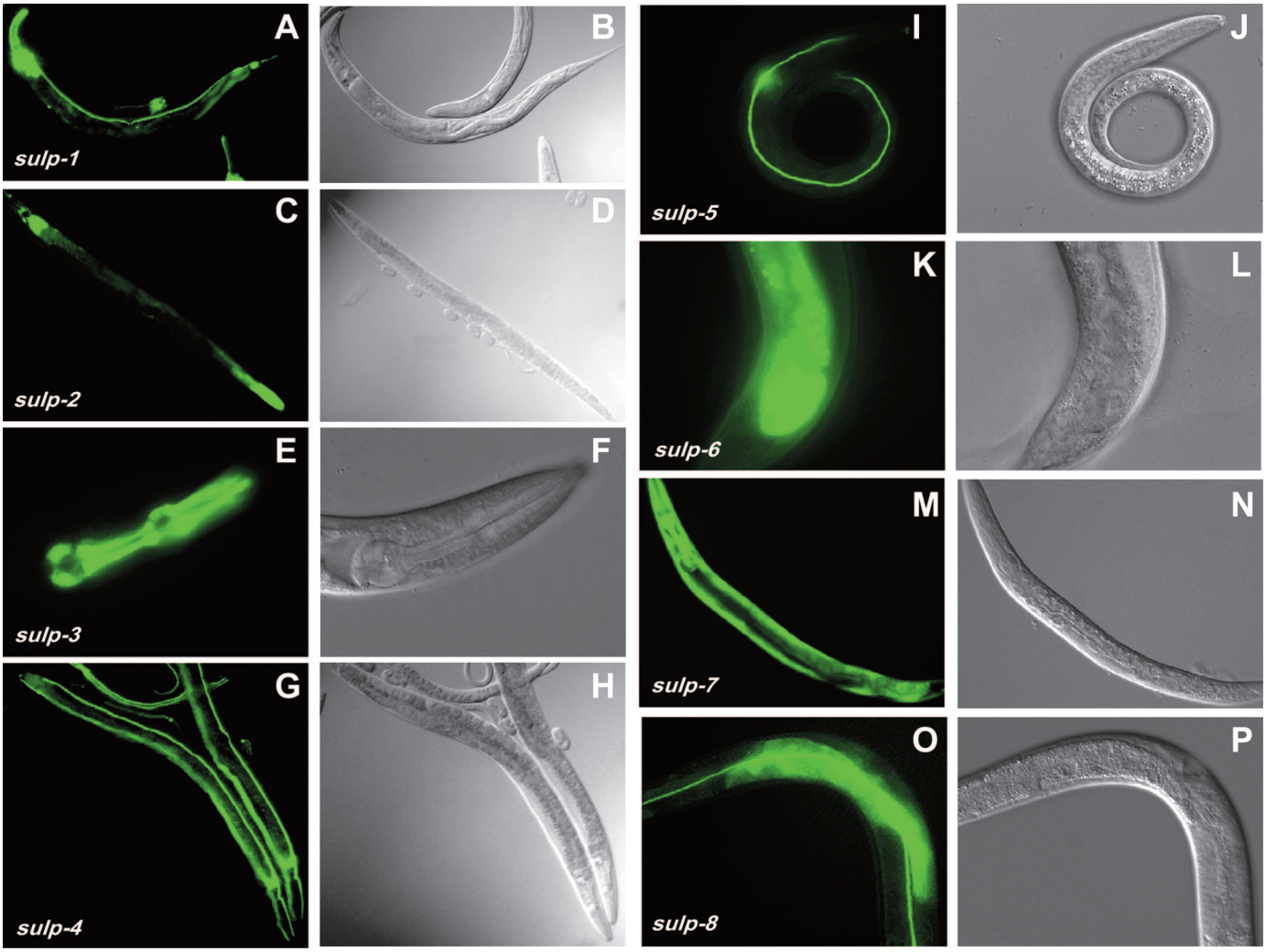

Fig. 3. Cell expression profiles of the *sulp* gene family: transcriptional GFP fusions. The *sulp-1* promoter drove GFP expression most strongly in neurons and more weakly in hypodermal and intestinal cells (*A* and *B*), with very faint expression in the excretory cell and body wall muscles (not shown). The *sulp-2* promoter was active in the intestine (strongly in both the anterior- and posterior-most cells), as well as in several neurons near the anterior pharynx, including the dorsal CEPD and ventral CEPV cephalic neurons (*C* and *D*). The *sulp-3* promoter restricted expression exclusively to the pharynx, including pharyngeal muscle (pm) segments pm3, pm4, pm5, pm6, and pm7 (*E* and *F*). Both the *sulp-4* and *sulp-5* promoters drove GFP expression in the excretory cell (*G–J*), while the *sulp-6* promoter was active primarily in the midgut (*K* and *L*). The *sulp-7* promoter fusion resulted in bright GFP fluorescence in many cells of hypodermal, endothelial, and muscular lineage (*M* and *N*). Finally, the *sulp-8* promoter limited GFP expression to the intestine and the excretory cell (*O* and *P*).

found at the basolateral membrane of the intestine (Fig. 5, *C* and *E*). In addition to its expression in the excretory cell, the *sulp-5* translation fusion was weakly expressed in adult seam cells, which overlie the excretory cell and serve as the junction between the main body of hypodermal cells (Fig. 5*I*).

SULP-2::GFP was expressed in a distribution nearly identical to that of SULP-8::GFP, the *sulp* gene product to which it is most similar (Fig. 5*A*). However, the *sulp-2* translational fusion was also expressed in the cephalic neurons, in which it localized to the sensillar endings in the nose (Fig. 5*B*). The SULP-2 translational fusion protein was also expressed in the anterior deirid (ADE) and posterior deirid (PDE) neurons, in which the protein accumulated at the deirid sensilla located within the alae on the lateral lines (data not shown). The cephalic, ADE, and PDE neurons are dopaminergic (62) and function redundantly to allow the basal slowing response ob-

Table 2. *Subcellular localization of the 3′ GFP gene fusions to anion transport protein coding regions*

Name	Fusion Type	Tissues	Localization
ABTS-2::GFP	Translation	Excretory cell, ovaries, single neuron	Basolateral
ABTS-4::GFP	Translation	Intestine, single pair of neurons in head	Basolateral
SULP-2::GFP	Translation	Intestine, cephalic neurons, rectal gland	Basolateral, sensory cilia
SULP-4::GFP	Translation	Excretory cell, head neurons	Apical
SULP-5::GFP	Translation	Excretory cell, seam cell (weakly)	Apical, punctate
SULP-8::GFP	Translation	Excretory cell, intestine, rectal gland	Basolateral

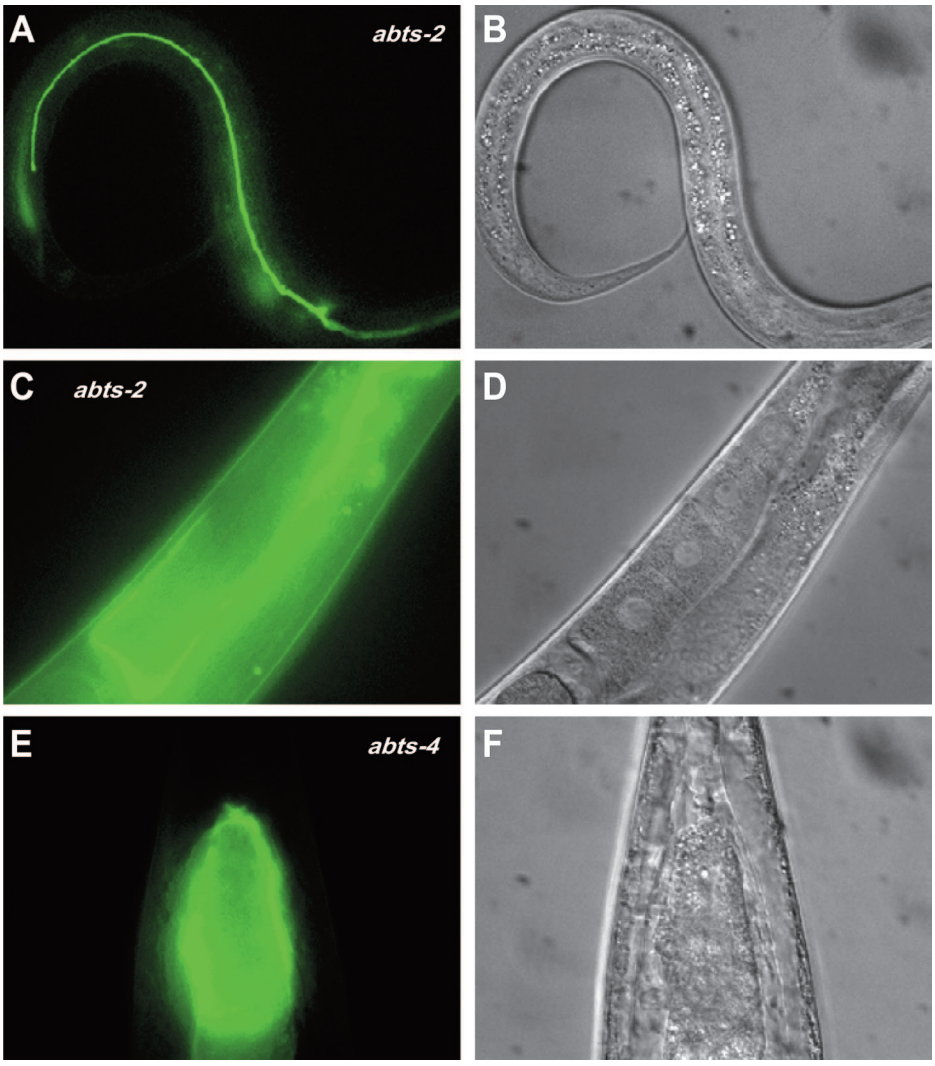

Fig. 4. Intracellular localization of the ABTS-2 and -4 proteins: translational GFP fusions. The promoters, along with the full genomic coding regions of both *abts-2* and *abts-4*, were fused in frame to GFP to localize proteins within cells. In contrast to the nonfusion GFP reporter (see Fig. 1*C*), the fusion protein ABTS-2::GFP was expressed in the excretory cell in the larvae (*A* and *B*) as well as in the ovaries in the adult (*C* and *D*) and was localized to the basolateral membrane of the excretory cell. The ABTS-4::GFP fusion was expressed on the basolateral membrane of the midgut, most strongly in the posterior intestinal cells (*E* and *F*).

served in response to refeeding after a brief period in the absence of food (52). Weak GFP expression in these neurons was observed in the transcriptional fusion as well (Fig. 3*C*).

Anion transport by ABTS and SULP proteins. The polypeptides encoded by the *abts* and *sulp* gene families are predicted to function as anion transporters. cRNA transcripts for ABTS-1, ABTS-2, SULP-2, and SULP-4 were injected into *Xenopus* oocytes. Anion influx assays were performed using Cl^-, sulfate, and oxalate as substrates. As shown in Fig. 6, SULP-4 exhibited robust transport of sulfate and more modest transport of Cl^- and oxalate, whereas ABTS-2 did not mediate detectable uptake of Cl^-, sulfate, or oxalate. The intestinal and neuronal SULP-2 exhibited modest uptake of sulfate. In contrast, the neuronal and hypodermal cell protein ABTS-1 exhibited robust Cl^- uptake without uptake of sulfate or oxalate (Fig. 6). ABTS-1 was therefore also examined for Cl^-/HCO_3^- exchange activity. As shown in Fig. 7, ABTS-1 conferred on *Xenopus* oocytes a 2.4-fold increase in Cl^-/HCO_3^- exchange activity.

DISCUSSION

Mammalian SLC4 AEs transport Cl^-, HCO_3^-, OH^-, and borate in both a Na^+-independent and a Na^+-dependent manner. Mammalian SLC26 AEs were originally identified as sulfate transporters, but SLC26 transporters more recently have been shown to transport a wide range of anions, including Cl^-, HCO_3^-, OH^-, oxalate, and formate. In polarized epithelial cells, most SLC4 AEs have been localized in basolateral membranes, but some reports of apical localization have been published. In contrast, SLC26 AEs more often have been localized to apical membranes, but several are found only basolaterally. Only SLC26 AEs interact functionally with CFTR.

To establish a genetically tractable model system in which to study AEs in the nematode *C. elegans*, we generated *C. elegans* cDNA encoding four *abts* polypeptides homologous to SLC4 AEs, and eight SULP polypeptides homologous to SLC26 AEs. We defined the cell type-specific expression patterns for these novel *C. elegans* polypeptides and documented functional anion transport activity for at least one member of each gene family. In combination with our previous studies of *C. elegans* NHEs, these results provide the foundation for the study of systemic acid-base physiology using the nematode model. Our results suggest that the molecular diversity of mammalian AEs is also present in worms. The four *C. elegans abts* genes correspond to nine mammalian *SLC4* genes. The eight *C. elegans sulp* genes

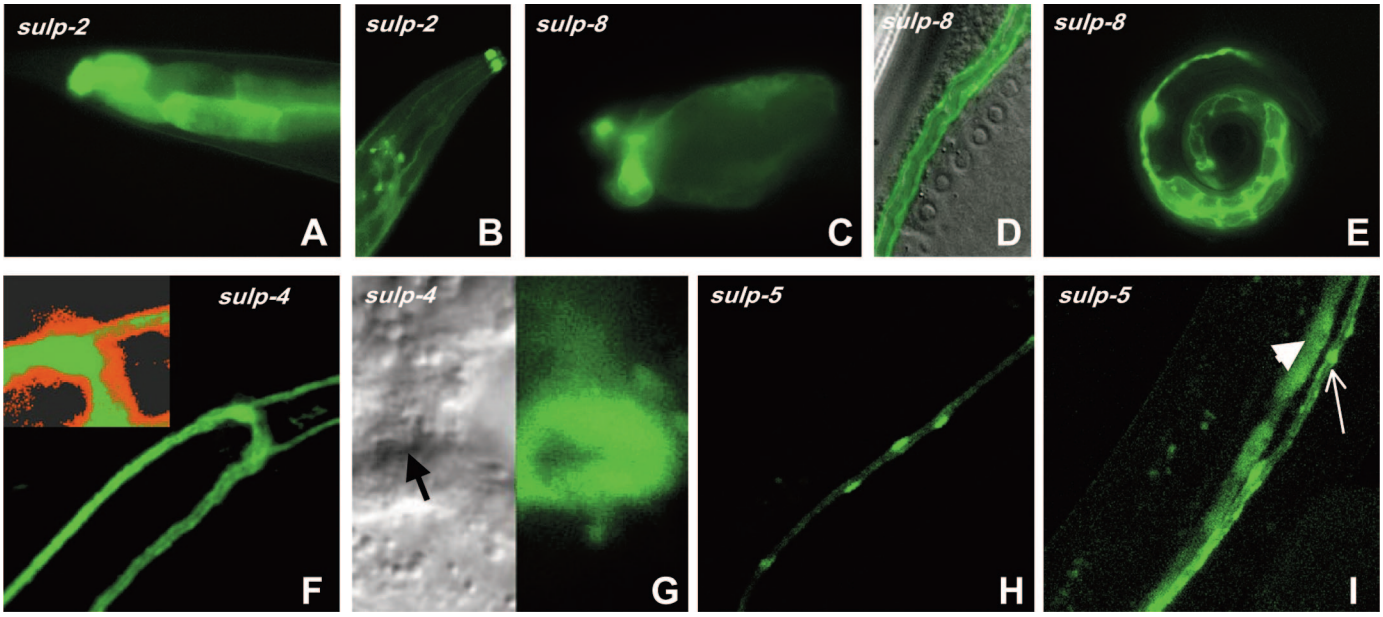

Fig. 5. Intracellular protein targeting of the *sulp* gene family: translational GFP fusions. SULP-2::GFP fusion protein was targeted to the basolateral membrane of the midgut and rectal gland cells (*A*) and to the tip of the cephalic sensory processes (*B*). SULP-8::GFP protein was also targeted to the basolateral membrane of the midgut and rectal gland cells (*C*), as well as to the excretory cell, as shown in an overlay using confocal microscopy (*D*). This targeting was readily apparent in a recently hatched L1 larva (*E*). In contrast, the SULP-4::GFP fusion protein was localized via confocal imaging to the canaliculae leading to the apical membrane of the excretory cell (*inset*: basolateral boundary of the cell delineated by red pseudocolor) (*F*). This is shown more clearly in a confocal cross section of the excretory canal near the cell body, where an arrow marks the lumen and the protein resides in the canalicular membrane (*G*). The SULP-5::GFP fusion protein is also targeted to the apical membrane, but with a focal, punctate distribution (*H*). Expression of SULP-5::GFP was variably noted in the seam cells of adult animals (arrowhead), as well as in the underlying excretory cell (arrow), as shown in a confocal Z series image stack (*I*).

correspond to 11 *SLC26* genes in mammals, one of which appears to be a pseudogene.

The *C. elegans abts* polypeptide sequences are not clearly orthologous to individual *SLC4* sequences, although the highest pairwise percentage amino acid identities were 50% between ABTS-1 and SLC4A8 and 38% between ABTS-3 and the mammalian borate transporter BTR1. BTR1 was recently described as the 11th member of the SLC4 superfamily and was termed NaBC1 to reflect electrogenic Na^+-coupled borate transport (43). BTR1 resembled ABTS-2, -3, and -4 more closely than it did any of the other mammalian slc4 isoforms. In addition, while there was a high degree of sequence relatedness between the Na^+-HCO_3^- cotransport arm of SLC4 and ABTS-1, the robust transport of Cl^- by ABTS-1 expressed in *Xenopus* oocytes may be more consistent with Na^+-dependent Cl^-/HCO_3^- exchange, such as that mediated by SLC4A8. In addition, the nematode proteins may display previously unrecognized or specialized functions.

Similarly, individual SULP polypeptides were not clear orthologs of single SLC26 polypeptides or subfamilies. The highest pairwise percentage amino acid identity was 33% between SULP-5 and SLC26A2, although the percentage amino acid similarity was ~50% between any given nematode polypeptide and human polypeptide.

Expression of the majority of these transporters was detected in polarized cell types, including the pharynx, the excretory cells, and the cells of the intestine (Table 1). Each of these cell types serves a specialized function in worms, and these functions may suggest physiological roles for these transporters. For example, because no hypodermal layer separates the pharyngeal muscle anchorage from the cuticle and the pharyngeal muscles display myoepithelial properties and participate in the secretion of cuticle, the *sulp-3* gene product might facilitate the accumulation of substrates for cuticle formation or in their export from the cell. Among these might be sulfate for sulfate proteoglycans and for the tyrosine sulfation apparently important for cuticular collagen cross linking (25) and (more speculatively) borate for cuticular glycan cross linking.

Laser ablation studies have shown that the excretory cell helps to maintain the osmolarity and volume of the pseudocoelom and that its loss leads to bloating and death within 24 h (40, 41). The expression of at least three *sulp* isoforms in the excretory cell supports the hypothesis that these SULP proteins enhance transepithelial electrolyte and fluid secretion from the pseudocoelom to the duct lumen.

Furthermore, intestinal expression of multiple *sulp* genes along with *abts-4* highlights the likely importance for this organ of anion transport and perhaps cellular and luminal pH regulation. Because electroneutral NaCl absorption in the mammalian intestine is mediated by parallel Na^+/H^+ and Cl^-/HCO_3^- exchange, it comes as no surprise that targeted genetic deletion of that apical enterocyte NHE3 leads to renal and intestinal absorptive deficits (53), while mutations in human *SLC26A3* cause congenital Cl^- diarrhea (18). Two of the three *C. elegans nhx* NHEs expressed exclusively in the intestine reside on the enterocyte apical membrane (39). We therefore hypothesized that the enterocyte apical membrane would harbor at least one of the newly identified anion transporter proteins. However, each of the three gene products identified in intestinal cells was localized to the basolateral membrane, and preliminary data suggest that the long isoform of *sulp-7* also encodes a protein targeted to the basolateral

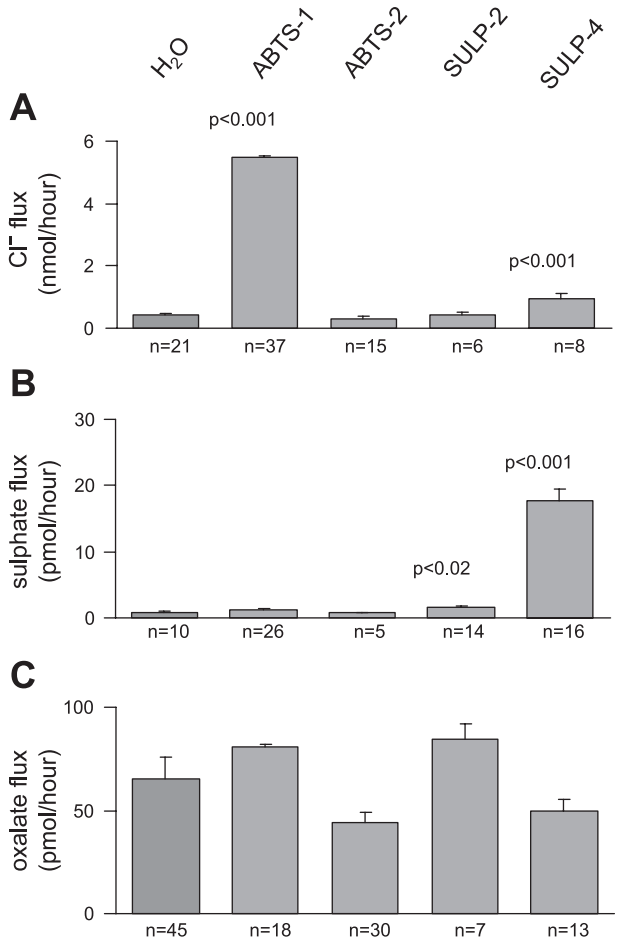

Fig. 6. Members of both the *abts* and *sulp* gene families mediate transmembrane anion flux. Recombinant cRNA encoding ABTS-1, ABTS-2, SULP-2, and SULP-4 were injected into *Xenopus* oocytes, and their activities were determined by measuring the influx of radiolabeled Cl^- (*A*) sulfate (*B*), or oxalate (*C*). The number (*n*) of injected oocytes measured under each condition is shown. Bars, SE. *P* values shown represent comparison with water-injected oocytes.

membrane (data not shown). Indeed, most of the GFP fusion polypeptides were localized basolaterally, which raises the possibility that they might be missorted, especially if normal sorting required integrity of the COOH-terminal PDZ recognition motif. Confirmation of these initial results will require the use of antibodies directed toward the native sequences. It remains possible that the *sulp-6* gene product, which could not be examined as a translational GFP fusion because of an incomplete cDNA 3′ end, may reside on the enterocyte apical membrane.

We also have shown that SULP-2 resides in the sensory cilia of ADE, PDE, and cephalic neurons. These dopaminergic neurons (62) cooperatively mediate the basal slowing response produced in well-fed worms by the reintroduction of food (52). Dopamine signaling modulates behavioral plasticity in *C. elegans* (50), and degeneration of these dopaminergic neurons has been studied in a worm model of Parkinson's disease. The restriction of neuronal SULP-2 expression to these three sets of functionally redundant cells suggests a possible role for SULP-2 related to dopaminergic function, and the link between neuronal and intestinal function may be significant. Because the roles of SLC4 and SLC26 AEs in mammalian neuronal function remain little understood (9), the study of *C. elegans* homologs may provide important insights.

Finally, we have shown that ABTS-2 and SULP-4 each mediate anion transport in *Xenopus* oocytes. Recombinant expression of ABTS-1 also results in detectable Cl^-/HCO_3^- exchange using a microelectrode approach to monitoring membrane voltage and pH_i (Romero M, unpublished observations). More extensive study of anion transport selectivity and optimization of functional expression systems will provide further insight to complement ongoing functional genetic studies.

The annotated genome and genetic tractability of the nematode model makes it particularly well suited to the study of integrative physiology (61). The transparency of the nematode allows for the use of transgenic fluorescent fusion proteins for real-time in vivo measurement of protein trafficking, pH_i (35), and intracellular cytoplasmic and/or organellar Ca^{2+} concentration (36). Advances in electrophysiological techniques have provided insights into electrogenic transport processes in the intact worm (14, 46), while the advent of embryonic cell culture has allowed comparative in vivo and in vitro study of identified single cells of defined lineage and developmental status (10). Together with the fast-growing repertoire of de-

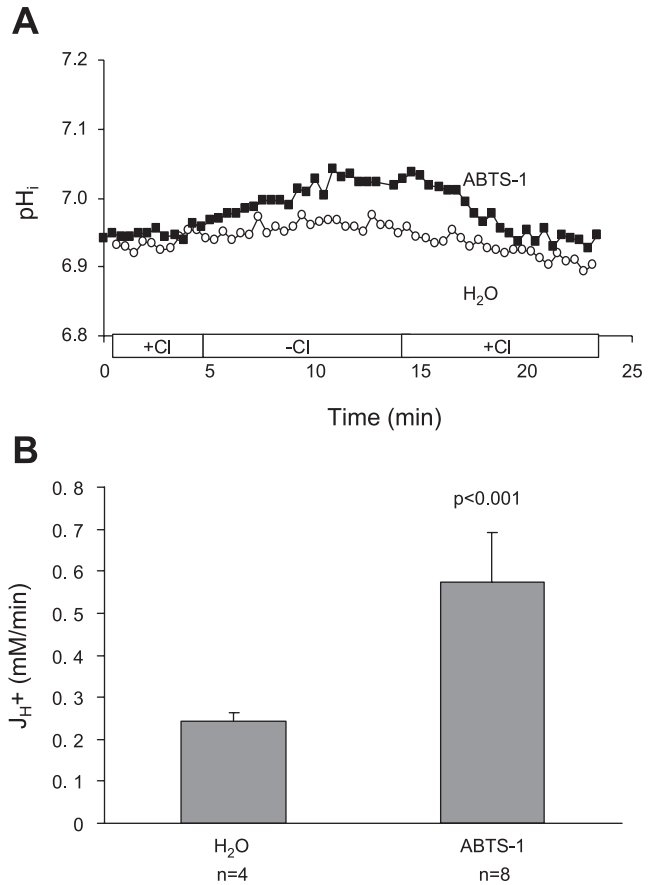

Fig. 7. ABTS-1 mediates Cl^-/HCO_3^- exchange. *A*: representative 2′,7′-bis-(2-carboxyethyl)-5-(and-6)-carboxyfluorescein acetoxymethyl ester-loaded oocytes previously injected with water or with *abts-1* cRNA were monitored for intracellular pH (pH_i) during bath Cl^- removal and restoration. *B*: ABTS-1 expression increased oocyte proton flux (J_{H^+}) attributable to Cl^-/HCO_3^- exchange. The number (*n*) of injected oocytes measured under each condition is shown. Bars, SD.

fined mutant strains, these experimental advantages facilitate direct physiological and biophysical study of individual ion transporters in the intact living organism. The data presented herein establish a model system for genetic studies of anion transport and acid-base physiology in the intact animal.

ACKNOWLEDGMENTS

We are grateful to the researchers at WormBase for compiling and annotating *C. elegans* genomic resources.

GRANTS

This work was supported in part by National Institutes of Health Grants DK-062763 and HL-08010 (to K. Nehrke) and National Institute of Diabetes and Digestive and Kidney Diseases Grants DK-43495 and DK-61051 (to S. L. Alper).

REFERENCES

1. **Alper SL.** Genetic diseases of acid-base transporters. *Annu Rev Physiol* 64: 899–923, 2002.
2. **Alper SL, Darman RB, Chernova MN, and Dahl NK.** The AE gene family of Cl/HCO_3^- exchangers. *J Nephrol* 15, *Suppl* 5: S41–S53, 2002.
3. **Aravind L and Koonin EV.** The STAS domain: a link between anion transporters and antisigma-factor antagonists. *Curr Biol* 10: R53–R55, 2000.
4. **Bissig M, Hagenbuch B, Stieger B, Koller T, and Meier PJ.** Functional expression cloning of the canalicular sulfate transport system of rat hepatocytes. *J Biol Chem* 269: 3017–3021, 1994.
5. **Bok D, Galbraith G, Lopez I, Woodruff M, Nusinowitz S, Beltrandel-Rio H, Huang W, Zhao S, Geske R, Montgomery C, Van Sligtenhorst I, Friddle C, Platt K, Sparks MJ, Pushkin A, Abuladze N, Ishiyama A, Dukkipati R, Liu W, and Kurtz I.** Blindness and auditory impairment caused by loss of the sodium bicarbonate cotransporter NBC3. *Nat Genet* 34: 313–319, 2003.
6. **Chernova MN, Jiang L, Crest M, Hand M, Vandorpe DH, Strange K, and Alper SL.** Electrogenic sulfate/chloride exchange in *Xenopus* oocytes mediated by murine AE1 E699Q. *J Gen Physiol* 109: 345–360, 1997.
7. **Chernova MN, Jiang L, Friedman DJ, Darman RB, Lohi H, Kere J, Vandorpe DH, and Alper SL.** Functional comparison of mouse slc26a6 anion exchanger with human SLC26A6 polypeptide variants: differences in anion selectivity, regulation, and electrogenicity. *J Biol Chem* 280: 8564–8580, 2005.
8. **Chernova MN, Jiang L, Shmukler BE, Schweinfest CW, Blanco P, Freedman SD, Stewart AK, and Alper SL.** Acute regulation of the SLC26A3 congenital chloride diarrhoea anion exchanger (DRA) expressed in *Xenopus* oocytes. *J Physiol* 549: 3–19, 2003.
9. **Chesler M.** Regulation and modulation of pH in the brain. *Physiol Rev* 83: 1183–1221, 2003.
10. **Christensen M, Estevez A, Yin X, Fox R, Morrison R, McDonnell M, Gleason C, Miller DM III, and Strange K.** A primary culture system for functional analysis of *C. elegans* neurons and muscle cells. *Neuron* 33: 503–514, 2002.
11. **Dahl NK, Jiang L, Chernova MN, Stuart-Tilley AK, Shmukler BE, and Alper SL.** Deficient HCO_3^- transport in an AE1 mutant with normal Cl^- transport can be rescued by carbonic anhydrase II presented on an adjacent AE1 protomer. *J Biol Chem* 278: 44949–44958, 2003.
12. **Everett LA, Glaser B, Beck JC, Idol JR, Buchs A, Heyman M, Adawi F, Hazani E, Nassir E, Baxevanis AD, Sheffield VC, and Green ED.** Pendred syndrome is caused by mutations in a putative sulphate transporter gene (*PDS*). *Nat Genet* 17: 411–422, 1997.
13. **Gawenis LR, Ledoussal C, Judd LM, Prasad V, Alper SL, Stuart-Tilley A, Woo AL, Grisham C, Sanford LP, Doetschman T, Miller ML, and Shull GE.** Mice with a targeted disruption of the AE2 Cl^-/HCO_3^- exchanger are achlorhydric. *J Biol Chem* 279: 30531–30539, 2004.
14. **Goodman MB, Hall DH, Avery L, and Lockery SR.** Active currents regulate sensitivity and dynamic range in *C. elegans* neurons. *Neuron* 20: 763–772, 1998.
15. **Granato M, Schnabel H, and Schnabel R.** *pha-1*, a selectable marker for gene transfer in *C. elegans*. *Nucleic Acids Res* 22: 1762–1763, 1994.
16. **Groves JD, Wang L, and Tanner MJA.** Functional reassembly of the anion transport domain of human red cell band 3 (AE1) from multiple and non-complementary fragments. *FEBS Lett* 433: 223–227, 1998.
17. **Hästbacka J, de la Chapelle A, Mahtani MM, Clines G, Reeve-Daly MP, Daly M, Hamilton BA, Kusumi K, Trivedi B, Weaver A, Coloma A, Lovett M, Buckler A, Kaitila I, and Lander ES.** The diastrophic dysplasia gene encodes a novel sulfate transporter: positional cloning by fine-structure linkage disequilibrium mapping. *Cell* 78: 1073–1087, 1994.
18. **Höglund P, Haila S, Socha J, Tomaszewski L, Saarialho-Kere U, Karjalainen-Lindsberg ML, Airola K, Holmberg C, de la Chapelle A, and Kere J.** Mutations of the Down-regulated in adenoma (*DRA*) gene cause congenital chloride diarrhoea. *Nat Genet* 14: 316–319, 1996.
19. **Humphreys BD, Chernova MN, Jiang L, Zhang Y, and Alper SL.** NH_4Cl activates AE2 anion exchanger in *Xenopus* oocytes at acidic pH_i. *Am J Physiol Cell Physiol* 272: C1232–C1240, 1997.
20. **Humphreys BD, Jiang L, Chernova MN, and Alper SL.** Functional characterization and regulation by pH of murine AE2 anion exchanger expressed in *Xenopus* oocytes. *Am J Physiol Cell Physiol* 267: C1295–C1307, 1994.
21. **Humphreys BD, Jiang L, Chernova MN, and Alper SL.** Hypertonic activation of AE2 anion exchanger in *Xenopus* oocytes via NHE-mediated intracellular alkalinization. *Am J Physiol Cell Physiol* 268: C201–C209, 1995.
22. **Igarashi T, Inatomi J, Sekine T, Cha SH, Kanai Y, Kunimi M, Tsukamoto K, Satoh H, Shimadzu M, Tozawa F, Mori T, Shiobara M, Seki G, and Endou H.** Mutations in *SLC4A4* cause permanent isolated proximal renal tubular acidosis with ocular abnormalities. *Nat Genet* 23: 264–266, 1999.
23. **Jiang L, Stuart-Tilley A, Parkash J, and Alper SL.** pH_i and serum regulate AE2-mediated Cl^-/HCO_3^- exchange in CHOP cells of defined transient transfection status. *Am J Physiol Cell Physiol* 267: C845–C856, 1994.
24. **Khurana OK, Coupland LA, Shelden MC, and Howitt SM.** Homologous mutations in two diverse sulphate transporters have similar effects. *FEBS Lett* 477: 118–122, 2000.
25. **Kim TH, Hwang SB, Jeong PY, Lee J, and Cho JW.** Requirement of tyrosylprotein sulfotransferase-A for proper cuticle formation in the nematode *C. elegans*. *FEBS Lett* 579: 53–58, 2005.
26. **Knauf F, Yang CL, Thomson RB, Mentone SA, Giebisch G, and Aronson PS.** Identification of a chloride-formate exchanger expressed on the brush border membrane of renal proximal tubule cells. *Proc Natl Acad Sci USA* 98: 9425–9430, 2001.
27. **Ko SBH, Shcheynikov N, Choi JY, Luo X, Ishibashi K, Thomas PJ, Kim JY, Kim KH, Lee MG, Naruse S, and Muallem S.** A molecular mechanism for aberrant CFTR-dependent HCO_3^- transport in cystic fibrosis. *EMBO J* 21: 5662–5672, 2002.
28. **Ko SBH, Zeng W, Dorwart MR, Luo X, Kim KH, Millen L, Goto H, Naruse S, Soyombo A, Thomas PJ, and Muallem S.** Gating of CFTR by the STAS domain of SLC26 transporters. *Nat Cell Biol* 6: 343–350, 2004.
29. **Kopito RR.** Molecular biology of the anion exchanger gene family. *Int Rev Cytol* 123: 177–199, 1990.
30. **Kopito RR and Lodish HF.** Primary structure and transmembrane orientation of the murine anion exchange protein. *Nature* 316: 234–238, 1985.
31. **Lamprecht G, Heil A, Baisch S, Lin-Wu E, Yun CC, Kalbacher H, Gregor M, and Seidler U.** The down regulated in adenoma (*dra*) gene product binds to the second PDZ domain of the NHE3 kinase A regulatory protein (E3KARP), potentially linking intestinal Cl^-/HCO_3^- exchange to Na^+/H^+ exchange. *Biochemistry* 41: 12336–12342, 2002.
32. **Lohi H, Kujala M, Kerkelä E, Saarialho-Kere U, Kestilä M, and Kere J.** Mapping of five new putative anion transporter genes in human and characterization of SLC26A6, a candidate gene for pancreatic anion exchanger. *Genomics* 70: 102–112, 2000.
33. **Lohi H, Lamprecht G, Markovich D, Heil A, Kujala M, Seidler U, and Kere J.** Isoforms of SLC26A6 mediate anion transport and have functional PDZ interaction domains. *Am J Physiol Cell Physiol* 284: C769–C779, 2003.
34. **Mello CC, Kramer JM, Stinchcomb D, and Ambros V.** Efficient gene transfer in *C. elegans*: extrachromosomal maintenance and integration of transforming sequences. *EMBO J* 10: 3959–3970, 1991.
35. **Miesenböck G, De Angelis DA, and Rothman JE.** Visualizing secretion and synaptic transmission with pH-sensitive green fluorescent proteins. *Nature* 394: 192–195, 1998.
36. **Miyawaki A, Llopis J, Heim R, McCaffery JM, Adams JA, Ikura M, and Tsien RY.** Fluorescent indicators for Ca^{2+} based on green fluorescent proteins and calmodulin. *Nature* 388: 882–887, 1997.

37. **Mount DB and Romero MF.** The SLC26 gene family of multifunctional anion exchangers. *Pflügers Arch* 447: 710–721, 2004.
38. **Nehrke K.** A reduction in intestinal cell pH_i due to loss of the *Caenorhabditis elegans* Na^+/H^+ exchanger NHX-2 increases life span. *J Biol Chem* 278: 44657–44666, 2003.
39. **Nehrke K and Melvin JE.** The NHX family of Na^+-H^+ exchangers in *Caenorhabditis elegans*. *J Biol Chem* 277: 29036–29044, 2002.
40. **Nelson FK, Albert PS, and Riddle DL.** Fine structure of the *Caenorhabditis elegans* secretory-excretory system. *J Ultrastruct Res* 82: 156–171, 1983.
41. **Nelson FK and Riddle DL.** Functional study of the *Caenorhabditis elegans* secretory-excretory system using laser microsurgery. *J Exp Zool* 231: 45–56, 1984.
42. **Oliver D, He DZZ, Klöcker N, Ludwig J, Schulte U, Waldegger S, Ruppersberg JP, Dallos P, and Fakler B.** Intracellular anions as the voltage sensor of prestin, the outer hair cell motor protein. *Science* 292: 2340–2343, 2001.
43. **Park M, Li Q, Shcheynikov N, Zeng W, and Muallem S.** NaBC1 is a ubiquitous electrogenic Na^+-coupled borate transporter essential for cellular boron homeostasis and cell growth and proliferation. *Mol Cell* 16: 331–341, 2004.
44. **Parker MD, Ourmozdi EP, and Tanner MJA.** Human BTR1, a new bicarbonate transporter superfamily member and human AE4 from kidney. *Biochem Biophys Res Commun* 282: 1103–1109, 2001.
45. **Paw BH, Davidson AJ, Zhou Y, Li R, Pratt SJ, Lee C, Trede NS, Brownlie A, Donovan A, Liao EC, Ziai JM, Drejer AH, Guo W, Kim CH, Gwynn B, Peters LL, Chernova MN, Alper SL, Zapata A, Wickramasinghe SN, Lee MJ, Lux SE, Fritz A, Postlethwait JH, and Zon LI.** Cell-specific mitotic defect and dyserythropoiesis associated with erythroid band 3 deficiency. *Nat Genet* 34: 59–64, 2003.
46. **Richmond JE and Jorgensen EM.** One GABA and two acetylcholine receptors function at the *C. elegans* neuromuscular junction. *Nat Neurosci* 2: 791–797, 1999.
47. **Romero MF, Fulton CM, and Boron WF.** The SLC4 family of HCO_3^- transporters. *Pflügers Arch* 447: 495–509, 2004.
48. **Rothstein A, Cabantchik ZI, and Knauf P.** Mechanism of anion transport in red blood cells: role of membrane proteins. *Fed Proc* 35: 3–10, 1976.
49. **Saier MH Jr, Eng BH, Fard S, Garg J, Haggerty DA, Hutchinson WJ, Jack DL, Lai EC, Liu HJ, Nusinew DP, Omar AM, Pao SS, Paulsen IT, Quan JA, Sliwinski M, Tseng TT, Wachi S, and Young GB.** Phylogenetic characterization of novel transport protein families revealed by genome analyses. *Biochim Biophys Acta* 1422: 1–56, 1999.
50. **Sanyal S, Wintle RF, Kindt KS, Nuttley WM, Arvan R, Fitzmaurice P, Bigras E, Merz DC, Hébert TE, van der Kooy D, Schafer WR, Culotti JG, and Van Tol HHM.** Dopamine modulates the plasticity of mechanosensory responses in *Caenorhabditis elegans*. *EMBO J* 23: 473–482, 2004.
51. **Satoh H, Susaki M, Shukunami C, Iyama K, Negoro T, and Hiraki Y.** Functional analysis of diastrophic dysplasia sulfate transporter: its involvement in growth regulation of chondrocytes mediated by sulfated proteoglycans. *J Biol Chem* 273: 12307–12315, 1998.
52. **Sawin ER, Ranganathan R, and Horvitz HR.** *C. elegans* locomotory rate is modulated by the environment through a dopaminergic pathway and by experience through a serotonergic pathway. *Neuron* 26: 619–631, 2000.
53. **Schultheis PJ, Clarke LL, Meneton P, Miller ML, Soleimani M, Gawenis LR, Riddle TM, Duffy JJ, Doetschman T, Wang T, Giebisch G, Aronson PS, Lorenz JN, and Shull GE.** Renal and intestinal absorptive defects in mice lacking the NHE3 Na^+/H^+ exchanger. *Nat Genet* 19: 282–285, 1998.
54. **Schweinfest CW, Henderson KW, Suster S, Kondoh N, and Papas TS.** Identification of a colon mucosa gene that is down-regulated in colon adenomas and adenocarcinomas. *Proc Natl Acad Sci USA* 90: 4166–4170, 1993.
55. **Shibagaki N and Grossman AR.** Probing the function of STAS domains of the *Arabidopsis* sulfate transporters. *J Biol Chem* 279: 30791–30799, 2004.
56. **Sly WS and Hu PY.** Human carbonic anhydrases and carbonic anhydrase deficiencies. *Annu Rev Biochem* 64: 375–401, 1995.
57. **Steck TL, Ramos B, and Strapazon E.** Proteolytic dissection of band 3, the predominant transmembrane polypeptide of the human erythrocyte membrane. *Biochemistry* 15: 1153–1161, 1976.
58. **Sterling D, Alvarez BV, and Casey JR.** The extracellular component of a transport metabolon: extracellular loop 4 of the human AE1 Cl^-/HCO_3^- exchanger binds carbonic anhydrase IV. *J Biol Chem* 277: 25239–25246, 2002.
59. **Stewart AK, Chernova MN, Shmukler BE, Wilhelm S, and Alper SL.** Regulation of AE2-mediated Cl^- transport by intracellular or by extracellular pH requires highly conserved amino acid residues of the AE2 NH_2-terminal cytoplasmic domain. *J Gen Physiol* 120: 707–722, 2002.
60. **Stewart AK, Kerr N, Chernova MN, Alper SL, and Vaughan-Jones RD.** Acute pH-dependent regulation of AE2-mediated anion exchange involves discrete local surfaces of the NH_2-terminal cytoplasmic domain. *J Biol Chem* 279: 52664–52676, 2004.
61. **Strange K.** From genes to integrative physiology: ion channel and transporter biology in *Caenorhabditis elegans*. *Physiol Rev* 83: 377–415, 2003.
62. **Sulston J, Dew M, and Brenner S.** Dopaminergic neurons in the nematode *Caenorhabditis elegans*. *J Comp Neurol* 163: 215–226, 1975.
63. **Vandorpe DH, Shmukler BE, Jiang L, Lim B, Maylie J, Adelman JP, de Franceschi L, Cappellini MD, Brugnara C, and Alper SL.** cDNA cloning and functional characterization of the mouse Ca^{2+}-gated K^+ channel, mIK1: roles in regulatory volume decrease and erythroid differentiation. *J Biol Chem* 273: 21542–21553, 1998.
64. **Vince JW and Reithmeier RAF.** Identification of the carbonic anhydrase II binding site in the Cl^-/HCO_3^- anion exchanger AE1. *Biochemistry* 39: 5527–5533, 2000.
65. **Wang Z, Wang T, Petrovic S, Tuo B, Riederer B, Barone S, Lorenz JN, Seidler U, Aronson PS, and Soleimani M.** Renal and intestinal transport defects in Slc26a6-null mice. *Am J Physiol Cell Physiol* 288: C957–C965, 2005.